Nanostructured Ti-WO_3 Thin Films for Gas Sensor Applications

Ravi Kumar R., Jabbar Khan P., Sampurna Rao D., Adilakshmi G. and Sivasankar Reddy A.*
Department of Physics, Vikrama Simhapuri University, Nellore-524324, Andhra Pradesh, INDIA
*akepati77@gmail.com

Abstract
In this work, undoped and Ti doped WO_3 nanostructured films were prepared on the glass substrate using the electron beam evaporation method and the films microstructural, structural, chemical and gas sensor properties were studied. Undoped WO_3 films show the presence of nanoflakes and the surface appears homogenous and smooth. The nanoflakes are turned into nanorings after doping the Ti into WO_3. The target gases were tested at room temperature (30°C) with the same concentration. The Ti-WO_3 sensor possesses excellent selectivity towards hydrogen gas compared to other gases.

Keywords: Thin films, Tungsten oxide, Electron beam evaporation, Nanostructure, Gas sensors.

Introduction

In recent years, the demand for gas sensors has greatly increased in different fields such as military, environmental protection, industries and civil fields[19]. Gas sensors detect diverse gases including asphyxiating gases, volatile organic compounds and irritating gases. The sensing materials play a key role in gas sensors, which could interact with target gases. The sensing materials properties such as surface microstructure, electronic properties, flexibility and compatibility with substrates improve the sensing performance of gas sensors. In the past few decades, metal oxide semiconductors (MOSs) such as SnO_2, ZnO, TiO_2, Fe_2O_3, InGaZnO, NiO, $CuAlO_2$ and WO_3 are generally applied as gas sensitive materials owing to their low cost, high transparency, easy fabrication method, reproducibility and high sensitivities[1,2,13,11].

Among these MOSs, tungsten oxide (WO_3) is one of the most promising materials due to its outstanding properties and it possesses a variety of applications like sensors, antibacterial coatings, batteries, electrochromic and photochromic and photocatalysis[4,5,9,16,17,21]. To enhance gas sensing properties, WO_3 is often modified with an adequate quantity of noble metals or transition metals[10,15]. WO_3 based thin films are prepared using several methods such as electron beam evaporation[8], sputtering[18], spray pyrolysis[7] and electrodeposition-assisted sol-gel method[20]. In this work, WO_3 and Ti-doped WO_3 nanostructured films were prepared by electron beam evaporation and the gas sensor properties were studied.

Material and Methods

The nanostructured tungsten oxide (WO_3) and Ti-doped tungsten oxide (Ti-WO_3) thin films were prepared by electron beam evaporation technique onto the glass substrates using high purity (99.99%) WO_3 and Ti-WO_3 pellets. Table 1 lists the parameters that were maintained during the film deposition process.

Characterization of nanostructured WO_3 and Ti-WO_3 films: The microstructure was investigated through scanning electron microscopy (SEM), while the structural characteristics of the films were assessed using an X-ray diffractometer (XRD). The chemical composition was analyzed using X-ray photoelectron spectroscopy (XPS).

Results and Discussion

Microstructure: The SEM images of undoped and Ti doped nanostructured WO_3 films are illustrated in fig. 1(a-d). Undoped WO_3 films show the presence of nanoflakes and the surface appears homogenous and smooth as in fig. 1(a) revealing the amorphous character of the films.

Table 1
The parameters maintained during the deposition of the undoped and Ti doped WO_3 films

S.N.	Parameters	WO_3 Films	Ti-WO_3 Films		
			5 wt%	10 wt%	15 wt%
1	Accelerating Voltage (kV)	48	48	48	48
2	Accelerating Current (mA)	1.3	1.3	1.3	1.3
3	Base Pressure (mbar)	3.8×10^{-6}	3.8×10^{-6}	3.8×10^{-6}	3.8×10^{-6}
4	Deposition Pressure (mbar)	1×10^{-3}	1×10^{-3}	1×10^{-3}	1×10^{-3}
5	Deposition Time (min)	10	12	12	12
6	Deposition Temperature	Room Temperature	Room Temperature	Room Temperature	Room Temperature

The nanoflakes are turned into nanorings and formed as clusters by adding the 5wt% of Ti to WO_3 as in fig. 1(b). On further increasing the dopant of Ti in WO_3 to 10wt%, the nanorings are clearly formed with some nanorods and clusters disappear as in fig. 1(c). The nanorings disappeared completely with the increase of the Ti content in WO_3 to about 15wt% and the microstructure appeared with uneven/random nanostructure with tiny nanorods as in fig. 1(d). These results indicate that Ti doping can lead to considerable microstructural changes in WO_3 films. In the literature, Cai et al[4] observed similar microstructural changes in template-free hydrothermal method Ti doped WO_3 films. The undoped films exhibited porous and nanoscale interconnecting network structures. The macroporous surface and star-like structures were formed after adding the Ti to WO_3.

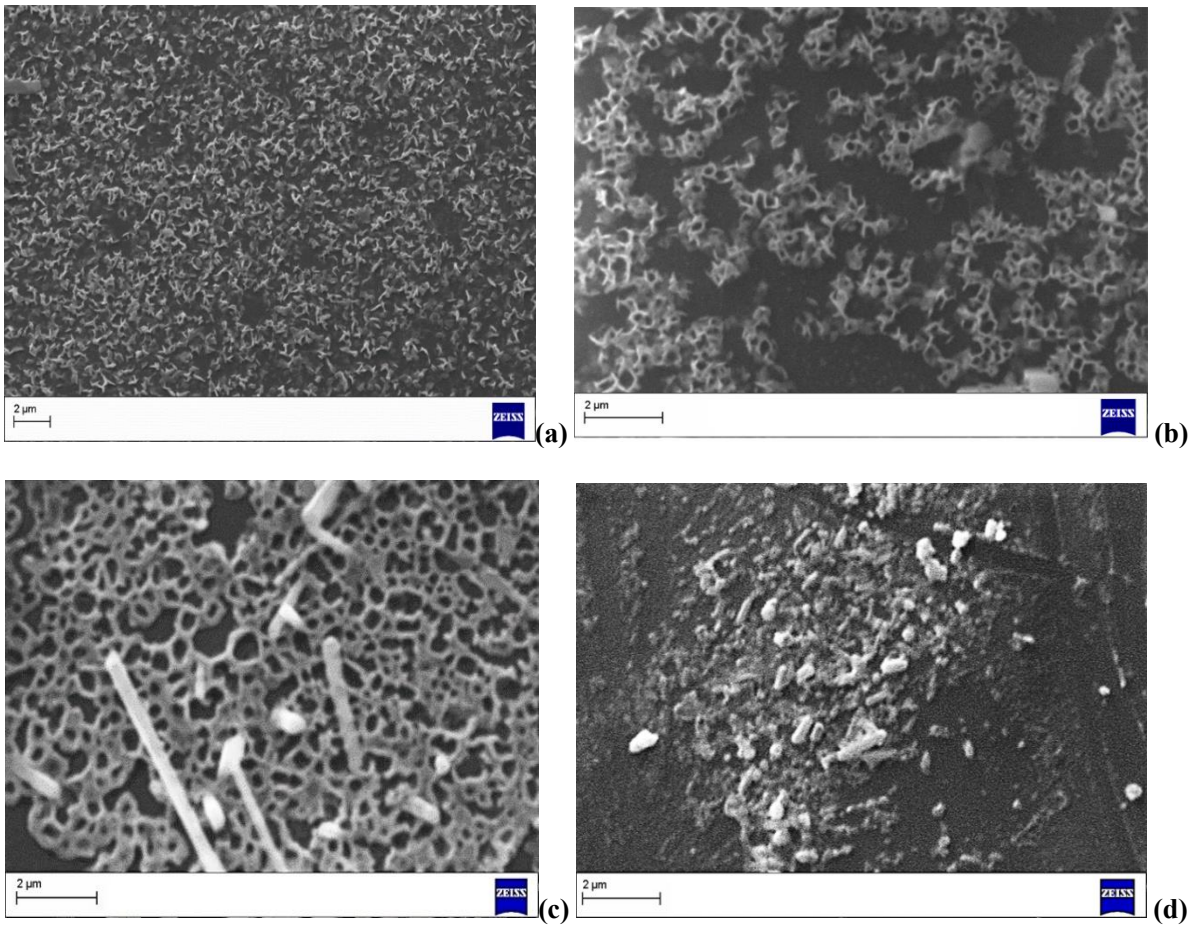

Fig. 1: SEM images of undoped and Ti doped WO_3 films: (a) undoped, (b) 5wt% Ti doped WO_3, (c) 10wt% Ti doped, WO_3 and (d) 15wt% Ti doped WO_3.

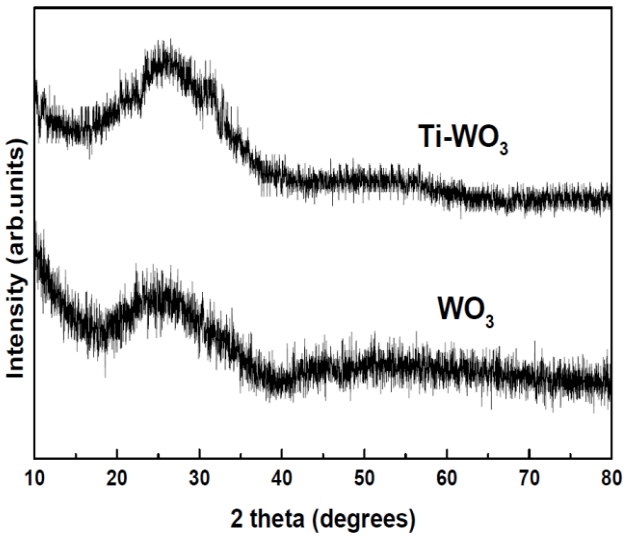

Fig. 2: XRD patterns of undoped and Ti doped WO_3 films: (a) undoped, (b) 10wt% Ti doped WO_3.

Structural analysis: The XRD patterns of the undoped and Ti doped WO_3 films are shown in fig. 2. The X-ray diffraction pattern of WO_3 films show no distinct diffraction peaks indicating amorphous in nature due to the low energy of tungsten oxide ions reaching the surface of the substrate and these low energy ions will prevent the crystallization of the WO_3 films. Consequently, the amorphous phase was obtained[14]. The addition of different wt% of Ti into WO_3 did not improve the crystal structure of WO_3 films and no peaks related to Ti, W, WO_3 or titanium oxide phases. Ti doping produces defect states, resulting in structural disorder in the WO_3.

The amount of defect states and structural disorder produced due to the doping of Ti may destabilize the WO_3 crystal structure leading to an amorphous structure. The broad hump appeared between diffraction angle 20° and 30° originating from the glass substrate[3].

XPS analysis: XPS is used to analyze the binding energy of the films and to identify trace elements of Ti doped WO_3 nanostructure films. Fig. 3(a-c) illustrates a typical XPS spectrum for the surface of a nanostructured 10wt% Ti doped WO_3 films and the films contained only the constituent elements such as W, O and Ti. Fig. 3 (a) shows the 4f spectrum of the WO_3. The spectrum doublets indicate the chemical states of tungsten (W) along with their associated binding energy peaks at 35.2 eV and 37.4 eV, corresponding to W 4f7/2 and W 4f5/2 respectively.

In fig. 3(b), the O 1s spectrum reveals a peak at 529.8 eV. In the context of transition metal oxides, two types of O 1s peaks can be identified: one associated with the O^{2-} peak in the range of 529.5 to 530.5 eV, which is characteristic of crystalline sites and the other peaks linked to O^- in the 531 to 532 eV range, typically found in sub-surface regions[6].

The Ti 2p XPS spectrum for the 10 wt% Ti-doped WO_3 film is illustrated in fig. 3(c) where it can be fitted with two doublets. Due to the relatively low concentration of Ti in the WO_3 matrix, the peaks are not distinctly resolved. The primary peak of the first doublet is located at 455.3 eV while the satellite peak appears at 463.6 eV, corresponding to Ti 2p3/2 and Ti 2p1/2 respectively.

Gas sensor properties: The gas sensing response was measured in a test chamber using a two-probe method to measure the film resistance. The measurement was conducted in a closed chamber that included a substrate heater and sample holder. Hydrogen and various alcohol vapors (ammonia, methanol, formaldehyde) were used as target gases to characterize the sensing capabilities of the undoped and Ti doped WO_3 sensors and the flow of gases monitored by the mass flow controller. The sample's operating temperature was controlled by a proportional-integral-derivative (PID) controller, connected to the heating component located at the rear of the sensor holder.

Selectivity is one of the important parameters of gas sensors. In this work, the selectivity of the gas sensor was analyzed by comparing the responses of hydrogen, ammonia, methanol and formaldehyde (Fig.4). All the target gases were examined at room temperature (30°C) with the same concentration. The Ti-WO_3 sensor possesses excellent selectivity for hydrogen gas compared to other target gases.

The important parameter for evaluating a sensor is to determine its optimum operating temperature. In this work, the sensor was examined within the operating temperature range of 30 °C-300 °C. Fig. 5 shows the effect of operating temperature on the hydrogen sensing behavior of 10wt% Ti doped WO_3 thin film. The resistance of gas sensing material decreased significantly with the increase in temperature. The present obtained resistance drop values are 4.35kΩ, 4.96kΩ and 3.70kΩ, for the operating temperatures of 30°C, 150°C and 300°C respectively.

By increasing the operating temperature, the target gas molecules became more and more active, consequently the resistance drop values are increased. At a higher operating temperature of 300°C, the resistance drop value is minimal due to the deterioration of the gas diffusion[12].

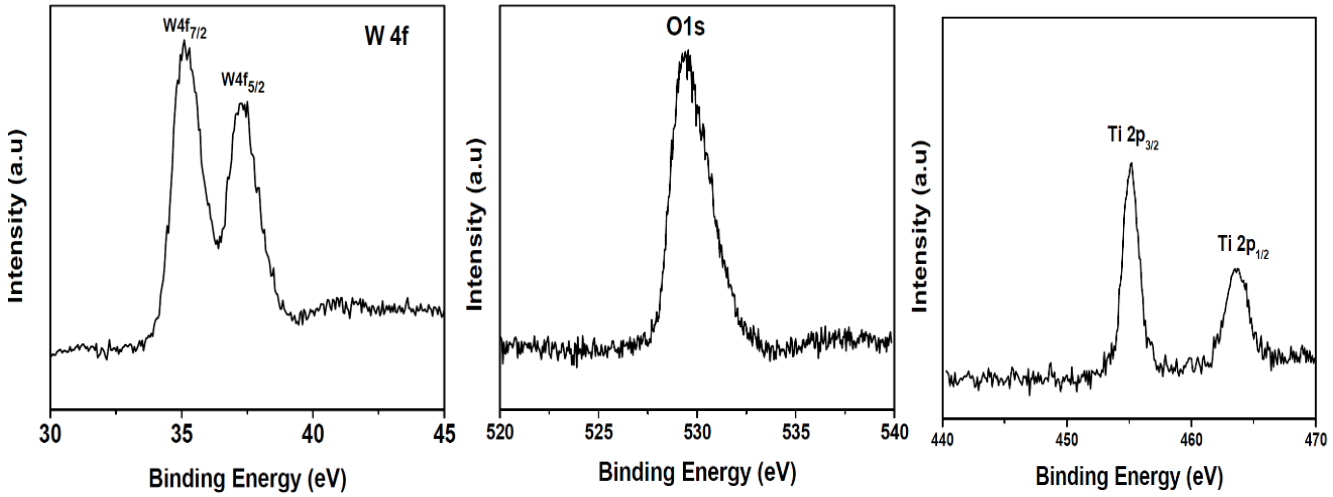

Fig. 3: XPS spectra of nanostructured 10wt% Ti doped WO_3 films.

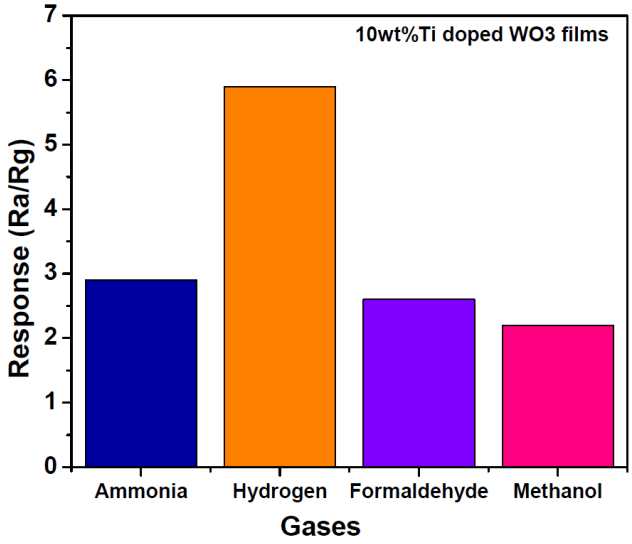

Fig. 4: Response of nanostructure 10wt% Ti doped WO_3 films at different gases.

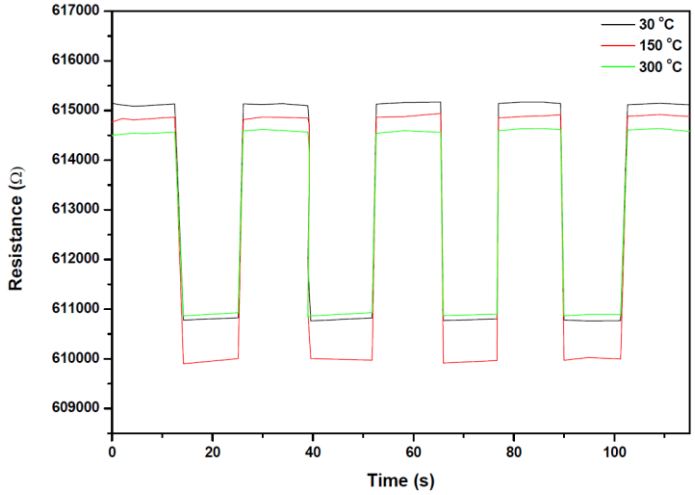

Fig. 5: Effect of operating temperature on the hydrogen sensing behavior of 10wt% Ti doped WO_3 thin film.

Conclusion

Undoped and Ti doped WO_3 nanostructured films were prepared on the glass substrate using the electron beam evaporation method and the microstructural, structural, chemical and gas sensor properties were studied. Undoped WO_3 films show the presence of nanoflakes and the surface appears homogenous and smooth. The nanoflakes are turned into nanorings after adding the 10wt% of Ti to WO_3. The X-ray diffraction pattern of undoped and Ti doped WO_3 films shows no distinct diffraction peaks, indicating amorphous in nature. XPS is employed to investigate the binding energy of the films and to identify trace elements of Ti doped WO_3 nanostructure films.

The films contained only the constituent elements such as W, O and Ti. The Ti-WO_3 sensor possesses excellent selectivity towards hydrogen gas compared to other gases. The resistance of gas sensing material decreased significantly with increasing operating temperature. The electron beam evaporated nanoring structured Ti doped WO_3 film is a simple and cost-effective way and can be used for gas sensor applications.

References

1. Arafat M.M., Dinan B., Akbar S.A. and Haseeb A.S.M.A., Gas Sensors Based on One Dimensional Nanostructured Metal-Oxides: A Review, *Sensors*, **12(6)**, 7207 **(2012)**

2. Berwal P., Rani S., Sihag S., Singh P., Bulla M., Jatrana A., Kumar A., Kumar A. and Kumar V., Fabrication of NiO based thin film for high-performance NO_2 gas sensors at low concentrations, *Physica B: Condensed Matter*, **685(15)**, 416023 **(2024)**

3. Bathe S.R. and Patil P.S., Titanium doping effects in electrochromic pulsed spray pyrolysed WO_3 thin films, *Solid State Ionics*, **179**, 314-323 **(2008)**

4. Cai G.F., Wang X.I., Zhou D., Zhang J.H., Xiong Q.Q., Gu C. and Tu J.P., Hierarchical structure Ti-doped WO_3 film with improved electrochromism in visible-infrared region, *RSC Advances*, **3(19)**, 6896 **(2013)**

5. Duan G., Chen L., Jing Z., Luna P.D., Wen L., Zhang L., Zhao L., Xu J., Li Z., Yang Z. and Zhou R., Robust Antibacterial Activity of Tungsten Oxide (WO_{3-x}) Nanodots, *Chem. Res. Toxicol.*, **32(7)**, 1357-1366 **(2019)**

6. Dupin J.C., Gonbeau C.D., Vinatier P. and Levasseur A., Systematic XPS studies of metal oxides, hydroxides and peroxides, *Phys. Chem. Chem. Phys*., **2(6)**, 1319-1324 **(2000)**

7. Ganbavle V., Shaikh S., Mohite S., Inamdar S., Bagade A., Patil A. and Rajpure K., Synergistic effects of Pd decoration and substrates on the NO_2 sensing performance of sprayed WO_3 thin films, *Chemical Physics Letters*, **814**, 40327 **(2023)**

8. Griddaluru A. and Akepati S.R., Electron beam evaporated gold doped tungsten oxide nanostructured films for sensor applications, *Chem Phys Mater*, **2(2)**, 172-179 **(2023)**

9. Hariharan V., Radhakrishnan S., Parthibavarman M., Dhilipkumar R. and Sekar C., Synthesis of polyethylene glycol (PEG) assisted tungsten oxide (WO_3) nanoparticles for l-dopa bio-sensing applications, *Talanta*, **85(4)**, 2166-2174 **(2011)**

10. Hu M., Wang W.D., Zeng P., Zeng J. and Qin Y.X., Density Functional Theory (DFT) calculations to explore the interaction of H2 with pure and Ti-doped WO3 (002) surfaces, *Chin. Phys. B*, **21(2)**, 02310 **(2012)**

11. Lee J.H., Technological Realization of Semiconducting Metal Oxide-Based Gas Sensors, Elsevier Inc., Amsterdam, 167–216 **(2018)**

12. Li Z., Yao Z.J., Haidry A.A., Plecenik T., Xie L.J., Sun L.C. and Fatima Q., Resistive-type hydrogen gas sensor based on TiO_2: A review, *Int. J Hydrogen Energy*, **43**, 21114 **(2018)**

13. Lin Y.F, Dong B.C., Liao S.Y., Chen B.R., Lin L.Z., Chang Y., Wu M.H., Su P.Y., Chen B.C., Hsueh W.J. and Huang C.Y., Highly sensitive and stable room-temperature gas sensors based on the photochemically activated p-type $CuAlO_2$ thin films, *Mater. Chem. Physics*, **309**, 128328 **(2023)**

14. Mazura M., Wojcieszak D., Wiatrowski A., Kaczmarek D., Luba´nska A., Domaradzki J., Mazur P. and Kalisz M., Analysis of amorphous tungsten oxide thin films deposited by magnetron sputtering for application in transparent electronics, *Applied Surface Science*, **570**, 15115 **(2021)**

15. Penza M., Martucci C. and Cassano G., NO_x gas sensing characteristics of WO_3 thin films activated by noble metals (Pd, Pt, Au) layers, *Sensors and Actuators B: Chemical*, **50(1)**, 52-59 **(1998)**

16. Ramkumar S.S. and Rajarajan G., Effect of Fe doping on structural, optical and photocatalytic activity of WO_3 nanostructured thin films, *J Mater Sci: Mater Electron*, **27**, 1847-1853 **(2016)**

17. Syed M.A., Manzoor U., Shah I. and Bukhari S.H., Antibacterial effects of Tungsten nanoparticles on the Escherichia coli strains isolated from catheterized urinary tract infection (UTI) cases and Staphylococcus aureus, *New Microbiol*., **33**, 329-35 **(2010)**

18. Usha K.S. and Lee S.Y., Rapid thermal annealing treatment on WO_3 thin films for energy efficient smart windows, *Ceramics International*, **50(13)**, 23244-23255 **(2024)**

19. Wang Z., Bu M., Hu N. and Zhao L., An overview on room-temperature chemiresistor gas sensors based on 2D materials: Research status and challenge, *Composites Part B: Engineering*, **248**, 110378 **(2023)**

20. Zeng J., Yan S., Bai J., Zhang Y., Yang G., Zhang D., Liu Z. and Liang X., Amorphous/ordered porous crystalline stacked WO_3 films fabricated by electrodeposition-assisted sol–gel and its application to electrochromic devices, *J. Electroanalytical Chemistry*, **952**, 117969 **(2024)**

21. Zhu W., Liu J., Yu S., Zhou Y. and Yan X., Ag loaded WO_3 nanoplates for efficient photocatalytic degradation of sulfanilamide and their bactericidal effect under visible light irradiation, *J. Hazard Mater.*, **318**, 407-416 **(2016)**.

(Received 06th March 2025, accepted 09th April 2025)